Chemistry & Biology, Vol. 11, 787–797, June, 2004, ©2004 Elsevier Ltd. All rights reserved. DOI 10.1016/j.chembiol.2004.04.008

Targeting Wide-Range Oncogenic Transformation via PU24FCl, a Specific Inhibitor of Tumor Hsp90

Maria Vilenchik,[1,4] David Solit,[1,4] Andrea Basso,[1,5] Henri Huezo,[1] Brian Lucas,[1,6] Huazhong He,[1] Neal Rosen,[1] Claudia Spampinato,[2] Paul Modrich,[2,3] and Gabriela Chiosis[1,*]

[1]Program in Cell Biology and Department of Medicine
Memorial Sloan-Kettering Cancer Center
New York, New York 10021
[2]Howard Hughes Medical Institute and
[3]Department of Biochemistry
Duke University Medical Center
Durham, North Carolina 27710

Summary

Agents that inhibit Hsp90 function hold significant promise in cancer therapy. Here we present PU24FCl, a representative of the first class of designed Hsp90 inhibitors. By specifically and potently inhibiting tumor Hsp90, PU24FCl exhibits wide-ranging anti-cancer activities that occur at similar doses in all tested tumor types. Normal cells are 10- to 50-fold more resistant to these effects. Its Hsp90 inhibition results in multiple anti-tumor-specific effects, such as degradation of Hsp90-client proteins involved in cell growth, survival, and specific transformation, inhibition of cancer cell growth, delay of cell cycle progression, induction of morphological and functional changes, and apoptosis. In concordance with its higher affinity for tumor Hsp90, in vivo PU24FCl accumulates in tumors while being rapidly cleared from normal tissue. Concentrations achieved in vivo in tumors lead to single-agent anti-tumor activity at non-toxic doses.

Introduction

Human cancer is characterized by genetic instability leading to the amplification or mutation of oncogenes. These genetic alterations may inhibit apoptosis, lead to dysregulated growth, or enhance metastatic potential. A number of genetic alterations responsible for the malignant phenotype have been identified, and a trend in cancer therapy over the past 10 years has been to develop agents that "target" a single molecular alteration. These efforts have led to the development of novel therapies such as Gleevec [1, 2] and Herceptin [3, 4], which have been successful for the small fraction of patients with tumors dependent on the oncoproteins they target. However, because most tumors are characterized by multiple growth regulatory alterations, targeting one abnormality is insufficient. In addition, because the growth-regulatory alterations are cell specific, a drug targeting one abnormality will be limited to use in only a subset of cancers. Identifying the subset of responsive tumors has been difficult in clinical trial settings, and many drugs have failed because of inadequate patient selection. Furthermore, the genetic plasticity of cancer cells often permits rapid development of resistance, even in patients who initially respond to targeted agents such as Gleevec [5].

It has been suggested that one potential way to circumvent this problem is to target the machinery that allows most cancer cells to function with the burden of abnormalities they carry: the molecular chaperone Hsp90 (see reviews [6, 7] by Neckers and Workman). Hsp90 is required for the ATP-dependent refolding of denatured or "unfolded" proteins and for the conformational maturation of a subset of proteins involved in the response of cells to extracellular signals. Activation of signaling pathways mediated by these Hsp90 clients is necessary for cell proliferation, regulation of cell cycle progression, and apoptosis. Additionally, gain-of-function mutations responsible for transformation often require Hsp90 for maintenance of their folded, functionally active conformations. Tumor Hsp90 is present entirely in multi-chaperone complexes with high ATPase activity, whereas Hsp90 from normal tissues is in a latent, uncomplexed state, suggesting that tumor cells contain Hsp90 complexes in an activated, high-affinity conformation that facilitates malignant progression [8].

These observations propose many potential clinical applications for agents that inhibit the chaperone activity of Hsp90. Unfortunately, currently reported Hsp90 inhibitors have not yet lived up to the promise of their target. Several natural products that have been identified as potently inhibiting Hsp90 (i.e., geldanamycin (GM) [9], herbimycin [10], and radicicol (RD) [11]; Figure 1) were restricted from clinical use because of in vivo toxicity and/or instability issues [10, 12]. A less toxic derivative of GM, 17-allylamino-17-demethoxygeldanamycin (17AAG) [13] (Figure 1), is currently in human clinical trials. This agent has activity in experimental tumor models [14, 15], and early clinical data are encouraging. However, 17AAG has several limitations, such as limited oral bioavailability and poor solubility. Furthermore, it is puzzling that several tumor models, such as Rb-defective tumors, which are sensitive to GM and RD, show partial or total resistance to 17AAG (D.S., unpublished data). Moreover, the dose-limiting toxicity of 17AAG in patients (liver toxicity) is likely attributable to the benzoquinone chemical structure of the compound and not to inhibition of Hsp90 [16]. Efforts to improve the solubility and bioavailability of 17AAG are underway (i.e., 17-dimethylaminoethylamino-17-demethoxygeldanamycin); however, the complex chemical structure of this class makes the search for derivatives with more drug-like properties very difficult, and it is improbable that future efforts will eliminate the benzoquinone feature of this compound without its losing activity.

Thus, the potential of Hsp90 as an anti-cancer target

*Correspondence: chiosisg@mskcc.org
[4]These authors contributed equally to this work.
[6]Present address: Department of Chemistry, University of Wisconsin, Madison, Wisconsin 53706.
[5]Present address: Department of Tumor Biology, Schering-Plough Research Institute, Kenilworth, New Jersey 07033.

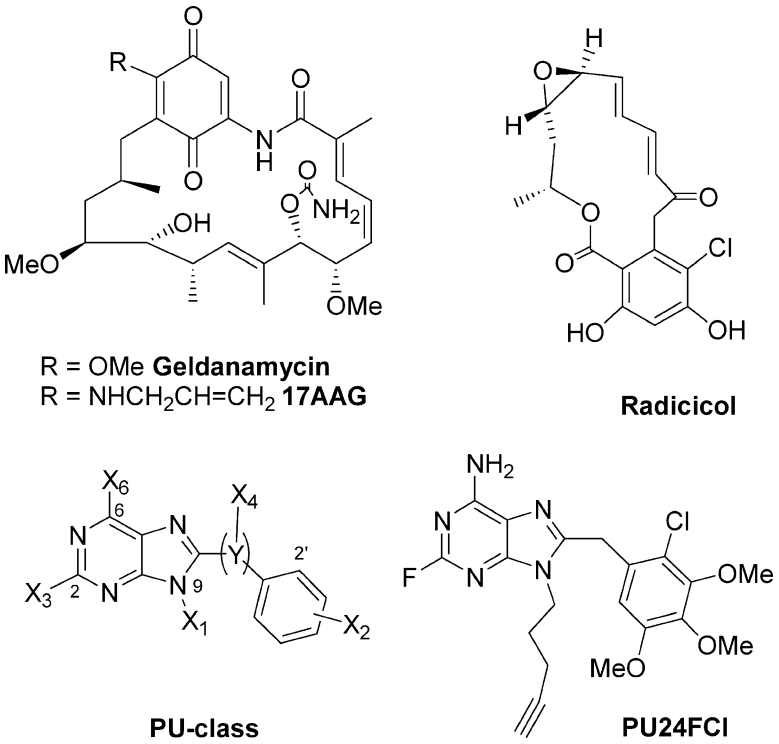

Figure 1. Chemical Structures of GM, 17AAG, RD, and the Designed PU Class of Hsp90 Inhibitors and Its Representative, PU24FCl

cannot be fully explored because of limitations of the existent inhibitors. To address that, we have developed a family of novel small molecules that potently and selectively inhibit Hsp90. We show here that one of these agents, PU24FCl, is highly specific for tumor Hsp90 and retains similar potency against a broad range of tumors in concordance with its inhibitory activity of tumor Hsp90. We also show that the agent manifests its anticancer activities via degradation of Hsp90 client proteins involved in tumor growth and survival, tumor-specific transformation, inhibition of cancer cell growth, delay of cell cycle progression, and induction of morphological and functional changes and apoptosis and that these occur at similar doses in all tested tumor types.

Results and Discussions

Design of the PU Class and Its Representative Lead Compound, PU24FCl

The N-terminal region of Hsp90 possesses a distinctive ATP/ADP binding pocket that is conserved from bacteria to mammals but is not present in other molecular chaperones [17]. When bound to the pocket, ATP and ADP adopt a C-shaped conformation found in other members of the superfamily of proteins called GHKL ATPases (G = DNA gyrase B, H = Hsp90, K = histidine kinase, L = MutL) but not observed in the high-affinity ATP/ADP binding sites [18–20]. Unlike protein kinases, which bind ATP/ADP with high affinity, Hsp90 binds these nucleotides with low affinity and has weak ATPase activity [21–23]. Thus, due to the unique structure of this pocket, an Hsp90 ligand has a priori a high chance for being specific.

We have previously defined the requirements for specific binding to the N-terminal pocket of Hsp90 [24]. We mentally distilled these requirements and designed the molecular class (PU class) illustrated in Figure 1 [25]. Rational changes in the variables X_1, X_2, and X_3 led to the development of PU24FCl (Figure 1) [26]. PU24FCl is a representative of this class and is by no means the most potent. In its design, empirical rules for solubility and cell permeability [27] and bioavailability [28] were additionally considered.

PU24FCl Is Highly Specific for Tumor Hsp90

In order to probe the affinity and specificity of PU24FCl for Hsp90, we tested its ability to compete with GM for binding to Hsp90 from tumor cells and also from normal tissues and organs. We used a homogeneous fluorescence polarization assay that can measure real-time interactions of cellular Hsp90 with the inhibitors. The apparent affinity of PU24FCl for tumor Hsp90 from several cellular lysates was relatively similar (an average relative binding affinity [EC_{50}] value of the six measured transformed cell lines of 0.22 $\pm$ 0.06 μM was calculated; Figures 2A and 2B). Although the agent bound tightly to Hsp90 found in transformed cells (breast cancer cell lines MCF-7, MDA-MB-468, and SKBr3, chronic myeloid leukemia cell line K562, and small cell lung cancers NCI-N417 and NCI-H69 are presented), its affinity for normal cell-Hsp90 was at least 10- (brain, pancreas and lung) to 50-fold lower (heart, kidney, and liver). Interestingly, PU24FCl's affinity for Hsp90 present in normal tissue was not only lower but also much more variable than for transformed cells (an average EC_{50} value for the six measured organs of 8.8 $\pm$ 7.6 μM was calculated) (Figure 2B). We were also able to confirm the previously reported higher affinity of 17AAG for tumor Hsp90 [8].

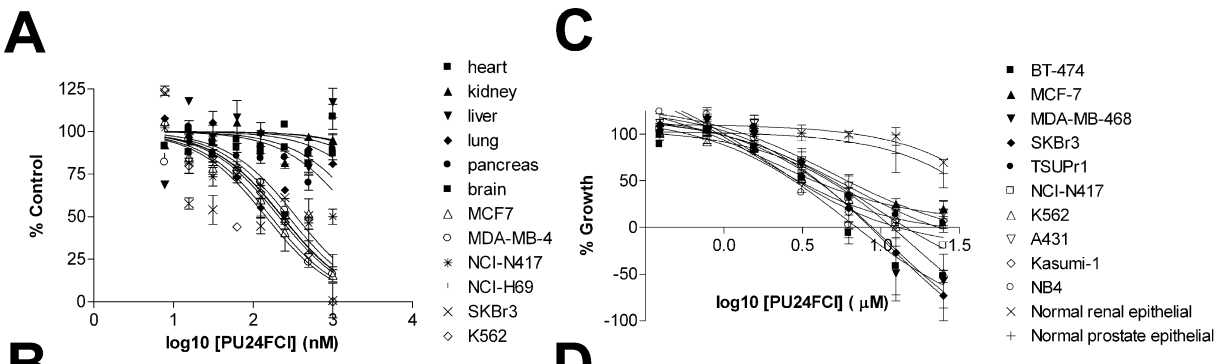

B

		EC_{50} Hsp90 inhibition (μM)
Normal	Heart	18.8±4.5
	Kidney	10.4±0.9
	Liver	16.8±3.9
	Lung	1.9±1.1
	Pancreas	2.7±0.7
	Brain	2.6±0.5
Transformed	MCF-7	0.22±0.07
	MBA-MD-468	0.23±0.02
	SKBr3	0.17±0.09
	K562	0.15±0.11
	NCI-N417	0.35±0.02
	NCI-H69	0.21±0.03

D

	Cell line	IC_{50} growth inhibition (μM)	IC_{50} total protein degradation (μM)		
			Raf-1*	**Akt***	**
Breast	**BT-474**	2.0±0.4	2.5	4	4 (**Her2**); 2 (**ER**)
	MCF7	4.5±0.7	2.6	2.5	
	MDA-MB-468	3.0±1.1	2.5	5	
	SKBr3	2.9±0.9	2.5	3	2 (**Her2**)
Prostate	**TSUPr1**	5.4±1.5	ND	ND	
	LNCaP	3.6±0.8	3	2.8	3.6 (**AR**)
AML	**Kasumi-1**	3.7±0.5	ND	ND	
	NB4	3.3±1.1	ND	ND	
Vulva	**A431**	7.2±0.8	3	3	
CML	**K562**	4.2±0.5	3	NA	4.5 (**Bcr-Abl**)
SCLC	**NCI-N417**	5.3±0.7	4	4	4 (**cMet**)
	NCI-H69	5.8±0.8	3.7	4	4 (**cMet**)
NSCLC	**A549**	2.9±1.1	2.5	2.7	
Colon	**Colo-205**	3.2±1.0	2.6	2.2	2.5 (**B-Raf**)
Neuroblastoma	**U87**	3.2±0.7	3.5	3	

Oncoproteins involved in cell growth/survival* and specific transformation**

Figure 2. PU24FCl's Potencies in Inhibiting Tumor Hsp90, Arresting the Growth of Tumor Cells, and Inducing the Degradation of Hsp90 Client Proteins Are Similar for All Tested Cell Lines

Normal tissue is 10-fold more resistant to PU24FCl's effects.

(A) The apparent affinity of PU24FCl for Hsp90 from several cell lysates was examined by a fluorescence polarization (FP) method that measures the ability of the agent to compete fluorescently labeled GM for Hsp90 binding.

(B) Relative binding affinity values (EC_{50}) obtained from FP measurements were determined, and data were presented.

(C) Effect of PU24FCl on the proliferation of a panel of transformed and normal cells. Cells were treated with drugs or vehicle for 72 hr as described in the Experimental Procedures. Determined IC_{50} values are presented in (D).

(D) PU24FCl induces the degradation of Hsp90 client proteins involved in tumor cell growth and survival and tumor-specific carcinogenesis at doses correlating with its ability to induce tumor growth arrest. Cells were treated with drugs or vehicle for 24 hr (for IC_{50} protein degradation) and 72 hr (for IC_{50} growth inhibition) as described in the Experimental Procedures, and proteins were analyzed by Western blot.

The EC_{50} values of 17AAG and GM for Hsp90 from several tumor cells were determined as follows: 14 ± 4 and 58.5 ± 20 nM in MCF-7, 39.8 ± 1.3 and 38.3 ± 9.4 nM in SKBr3, and 59 ± 7 and 37.5 ± 14 nM in MDA-MB-468, respectively. We tested GM for binding to Hsp90 from brain and obtained an EC_{50} of 850 ± 40 nM (in concordance with the 400 nM reported for 17AAG [8]). Our results do not corroborate the previous finding that tumor Hsp90 from Her2-overexpressing cells (i.e., SKBr3) confers a higher affinity for 17AAG than Hsp90 found in other cancer cells [8]. We also found 17AAG to be actively and potently binding to tumor Hsp90 from the SCLC cell lines NCI-H69 (EC_{50} of 15 ± 5 nM) and NCI-N417 (EC_{50} of 49 ± 10 nM). When compared to SKBr3, these tumors are at least 100 times more resistant to the anti-cancer actions of this drug. Thus, we cannot substantiate a direct link between Hsp90 affinity and cellular potency in the ansamycin class of compounds and propose that other factors may be responsible for the highly variant response of tumor cells to 17AAG [16, 29].

MutL is another mammalian GHKL member and is a protein involved in mismatch repair [20, 30, 31]. Because the ATPase centers of bacterial and eukaryotic MutL homologs are similar, we have evaluated PU24FCl and 17AAG for their effects on the well-characterized, single-strand, DNA-stimulated ATP-hydrolytic activity of *E. coli* MutL [30, 31]. MutL ATPase activity was relatively insensitive to inhibition by these agents at concentrations as high as 5 mM. Previously, 17AAG has been reported to bind with nanomolar affinity to ADE2 SAICAR purine synthetase, an enzyme involved in purine metabolic processing. The consequences of this effect are not completely understood, but it may be the cause of some in vivo toxicities of the drug. PU24FCl did not inhibit ADE2 enzyme activity at concentrations as high as 1 mM (V.J. Davisson, personal communication; determined IC_{50} = 2.2 mM). PU24FCl was also inert against a panel of kinases (Akt, Her2, Src, and EGFR) at concentrations as high as 100 μM.

PU24FCl Equivalently Affects Multiple Aspects of Transformation via Potent and Selective Inhibition of Tumor Hsp90 Activity

Inhibition of Cell Growth

We evaluated the in vitro growth-inhibitory properties of PU24FCl against a broad panel of cancer cell lines and two normal epithelial cells. Breast, prostate, acute

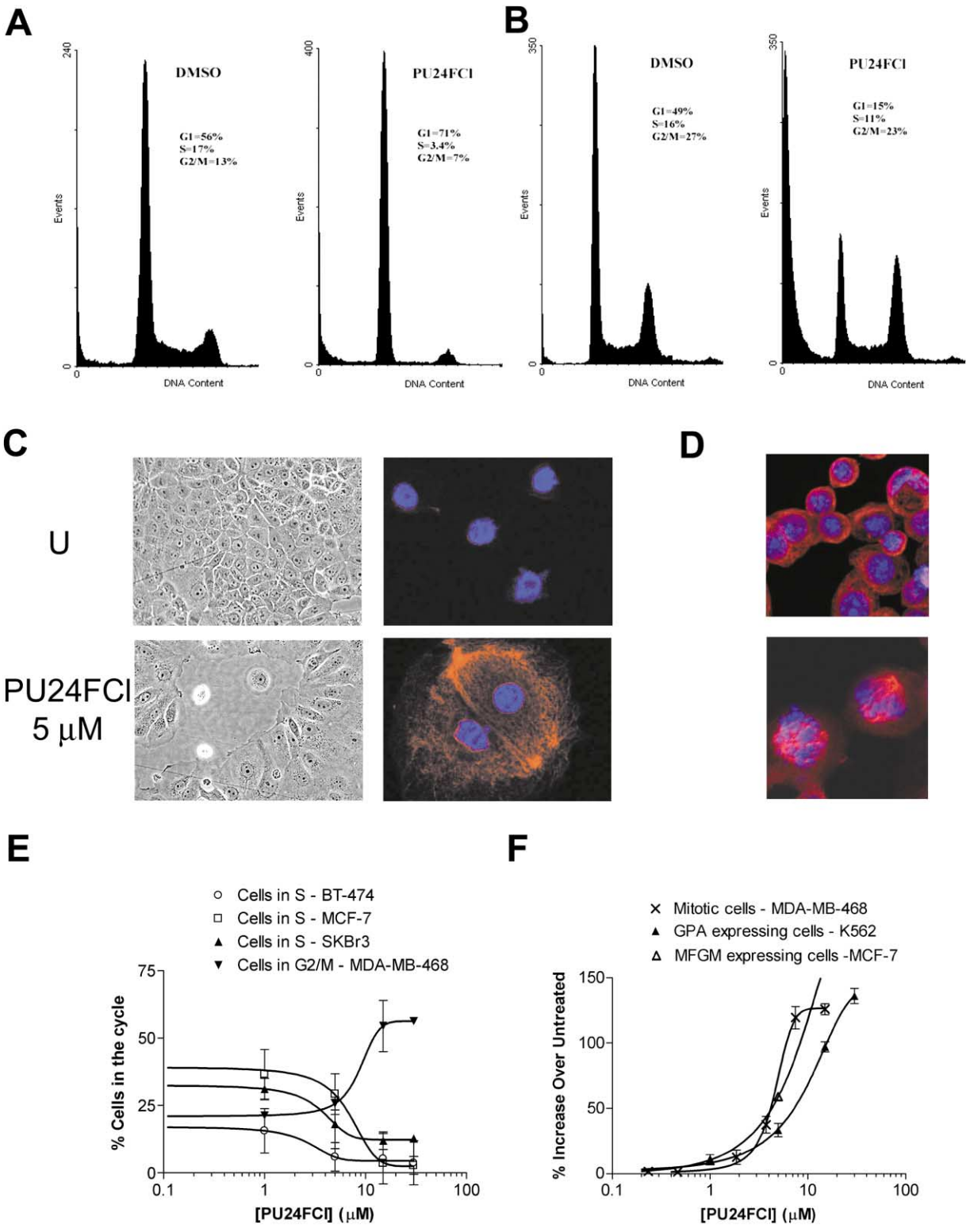

Figure 3. The Effects of PU24FCl on Cell Cycle Progression Are Specific to Cell Type but Occur at Similar Concentrations for All Tested Cancer Cell Lines, in Correlation with Its Other Hsp90-Dependent Activities

(A and B) Treatment of SKBr3 cells with PU24FCl induces a G1 arrest (A), whereas in MDA-MB-468 cells arrest occurred in G2/M (B). Cells were treated for 72 hr with 10 μM PU24FCl and stained with ethidium bromide before FACS analysis, as described in the Experimental Procedures.

(C) MCF-7 cells undergo morphological (left panel) and functional differentiation (right panel, induction of MFGM protein is presented) when they are treated with PU24FCl. Cells were treated for 48 hr with the indicated drug concentrations, and MFGM was detected with a mouse

myeloid leukemia (AML), acute promyelocytic leukemia, chronic myeloid leukemia (CML), colon, small cell lung cancer (SCLC), non-small cell lung cancer (NSCLC), and neuroblastoma cell lines and a vulvar squamous cell line were treated with PU24FCl for 72 hr, and the effects on cell viability were determined. PU24FCl inhibited cell proliferation and retained similar activity in all cancer cell lines tested. The IC_{50} values calculated after exposure to PU24FCl ranged from 2 to 7 μM (Figures 2C and 2D). The effects of PU24FCl appeared to be cytostatic in most tested cancer cell lines but cytotoxic in Her2-overexpressing cells (i.e., SKBr3 and BT-474, breast), Rb-defective cells (i.e., MDA-MB-468, breast and NCI-N417, SCLC) and in a bcr-abl-driven CML cell line (K562) (Figure 3A). By contrast to transformed cells, normal prostate epithelial cells (PrEC) (IC_{50} = 43.5 ± 5.3 μM) and human renal proximal tubular epithelial (RPTEC) (IC_{50}=63.5 ± 3.5 μM) were 1 log more resistant to the effects of PU24FCl on growth (Figure 2C), consistent with the 10- to 50-fold-higher affinity of this agent for tumor versus normal tissue Hsp90 (Figures 2A and 2B). PU24FCl retained activity in Rb-defective cancer cells. In these cells, such as SCLC cell lines (i.e., NCI-H69, NCI-N417) and certain breast cancer cells, such as MDA-MB-468, 17AAG is almost 2 log less sensitive than in most other cell lines (D.S., unpublished results and [33]). The cause of lack of potency in these cells is not Hsp90 dependent because the agent potently inhibits Hsp90 from these tumors (see above) and the phenomenon is not observed with PU24FCl.

Degradation of Hsp90 Client Proteins Involved in Cell Growth and Survival and Tumor-Specific Transformation

The effects of PU24FCl on growth were correlated with its effects on Hsp90 client proteins. These proteins (i.e., Her2, cMet, Raf-1, Akt, ER, mutant AR, mutant p53, and Bcr-Abl) are thought to be involved in the dysregulated growth potential and survival of tumor cells and to drive or contribute to transformation in many tumor types. Their levels 24 hr after treatment were determined by Western blot (Figure 2D). Degradation of these Hsp90 client proteins occurred at similar concentrations in the panel of cancer cells tested, in concordance with the similar affinity of the drug for the chaperone in these tumor cells (Figure 2A and data not shown). A significant reduction was observed for most Hsp90 client proteins as early as 8 hr after treatment, whereas no changes in PI3K (p85 unit) and β-actin, proteins not chaperoned by Hsp90, were observed (data not shown).

Arrest of the Cell Cycle by PU24FCl Is Specific to Cell Type but Occurs at Similar Doses in All Transformed Cell Lines

To evaluate the effect of PU24FCl on cell cycle progression, we tested a panel of tumor cell lines. The agent induced most cells to undergo growth arrest in G1 (Figure 3A), but others underwent arrest in G2/M (Figure 3B). The ability of the agent to block cells in the cell cycle was concentration dependent, with effects starting at 1 μM and reaching a maximum at 10 μM (Figure 3E) in agreement with its tumor Hsp90-related effects. G1 block in PU24FCl-treated cells was followed by morphological and functional differentiation (Figure 3C). MCF-7 breast cancer cells flattened, increased in size, and gained distinctive cellular boundaries upon treatment with PU24FCl (Figure 3C). Additionally, these cells underwent functional differentiation and reversal of transformation in the presence of the drug, as demonstrated by an induction of milk fat globule membrane protein (MFGM) [33] (Figure 3C). Another example of a cell line that differentiated upon PU24FCl addition is K562, a chronic myeloid leukemic cell line. GPA is a differentiation marker selectively expressed on the cell surface of erythroblast or erythroleukemia cells [34]. Treatment of K562 with PU24FCl caused a dramatic increase of GPA-expressing K562 cells (Figure 3F) at concentrations of PU24FCl above the growth inhibitory IC_{50} for this cell line. At such concentrations of RD, only a maximal 20% GPA induction was reported [35]. A tumor cell subset including all of those with defective Rb function (i.e., MDA-MB-468, NCI-N417, and NCI-H69), was resistant to induction of G1 block by PU24FCl and was blocked in mitosis (Figure 3D). The appearance of mitotic nuclei in the Rb-defective breast cancer cell line MDA-MB-468 occurred below 5 μM (Figure 3F), again in correlation with other anti-cancer effects of the agent in MDA-MB-468 (Figures 2C and 2D).

Induction of Apoptosis

Cell cycle arrest by PU24FCl was followed by apoptosis. The degree of apoptosis was cell type dependent (Figure 4A) but, as observed in Figure 4B, occurred at agent concentrations that produce all other Hsp90-related anti-cancer effects of PU24FCl. A significant increase in the number of apoptotic nuclei was observed in Her2-overexpressing (i.e., SKBr3; 19%) and Rb-defective (i.e., MDA-MB-468 and NCI-N417; 44% and 35%, respectively) cells at 72 hr after treatment.

In Vivo Effects of PU24FCl—Accumulation of Drug in Tumors Leads to Anti-Cancer-Effective Concentrations

Pharmacokinetic Analysis

The plasma concentration-time profile of PU24FCl after intraperitoneal (IP) and intravenous (IV) administration was determined. PU24FCl concentrations declined in an exponential fashion with a rapid absorption and distribution (Figure 5A). A 70 mg/kg IV and IP dose resulted in maximum plasma concentrations of 27.4 ± 5.9 μg/ml (63.1 ± 1.4 μM) and 5.2 ± 0.9 μg/ml (11.8 ± 0.2 μM),

primary antibody and rhodamine-labeled secondary antibodies. Nuclear DNA was stained with DAPI. Results were visualized, imaged, and quantified under confocal microscopy for immunofluorescence and under a light microscope for measurement of morphology change.

(D) The Rb-defective cell line MDA-MD-468 undergoes mitotic block when treated with PU24FCl. After a 24 hr treatment with vehicle or 5 μM PU24FCl, cells were stained with an anti-α-tubulin antibody as well as 1 μg/ml DAPI. Results were visualized, imaged, and quantified under confocal microscopy.

(E and F) Arrest in the cell cycle and induction of differentiation by PU24FCl are specific to cell type but occur at similar doses in all tested cell lines. (E) The increase in the number of mitotic cells (MDA-MB-468), GPA-expressing cells (K562), and MFGM-expressing cells (MCF-7) is presented as a function of PU24FCl concentration. See Experimental Procedures for more details.

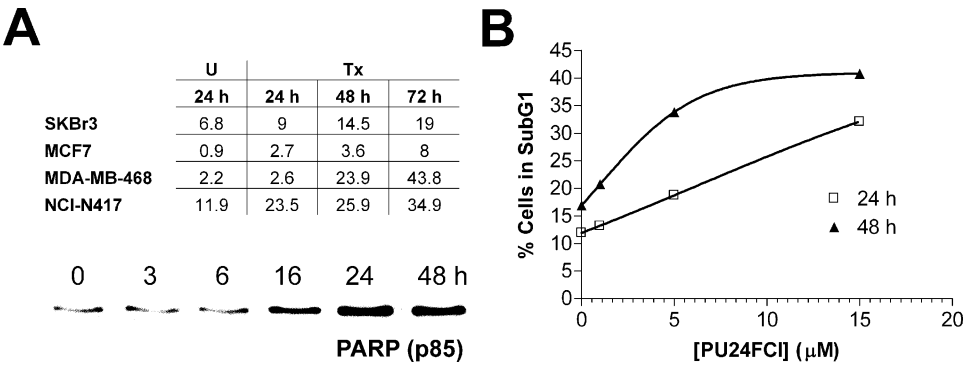

Figure 4. Cell-Specific Induction of Apoptosis by PU24FCl Occurs at Doses that Are in Correlation with Its Other Anti-Cancer Effects

(A) A cell cycle block in PU24FCl (10 μM)-treated cells is followed by apoptosis as determined by FACS analysis (%SubG1) and PARP cleavage (presented for SKBr3 cells). Cells were harvested at the indicated time periods and stained with ethidium bromide for FACS analysis, and PARP cleavage was analyzed by Western blot.

(B) A dose-dependent profile for induction of apoptosis in the SCLC cell line NCI-N417 by PU24FCl is presented. Figures portray data for a representative experiment. Analyses were reproduced at least twice.

which decreased to 0.6 ± 0.1 μg/ml (1.3 ± 0.2 μM) and 0.3 ± 0.1 μg/ml (0.7 ± 0.05 μM) 4 hr after administration, respectively. The calculated apparent volumes (2.84 $L \cdot kg^{-1}$ for IV and 13.55 $L \cdot kg^{-1}$ for IP) suggest that the agent is rapidly distributed after administration. There was no significant difference in the mean area-under-curve (AUC) values after IV and IP doses (561.8 $\mu g \cdot min \cdot ml^{-1}$ and 420.5 $\mu g \cdot min \cdot ml^{-1}$), resulting in an absolute bioavailability value (for IP administration) of approximately 75%. A long-term follow-up of PU24FCl distribution (200 mg/kg IP) suggested that, although the agent is quickly cleared from blood and normal tissue (brain and liver are presented), it is accumulated in tumor tissue with a maximum peak of 14.4 μM recorded 24 hr after administration (Figure 5B). An $AUC_{6-48\ hr}$ of 221.6 $\mu M \cdot min \cdot ml^{-1}$ was observed for tumor tissue, suggesting that the in vitro effective dose of 10 μM (IC_{90} for most cancer cells) was maintained in tumors for approximately 10 hr (20–30 hr after administration). The $AUC_{6-48\ hr}$ values for blood and normal tissue were recorded as 0.98 $\mu M \cdot min \cdot ml^{-1}$ for serum, 8.9 $\mu M \cdot min \cdot ml^{-1}$ for liver, and 0.3 $\mu M \cdot min \cdot ml^{-1}$ for brain. The highest concentrations in these tissues were 0.06, 0.67, and 0.01 μM, respectively, with values declining sharply after 12 hr. These values suggest that in the interval of 6–48 hr after administration, PU24FCl is mostly distributed to tumors (226, 25, and 753 times more than in blood, liver, and brain, respectively). They also hint to breakdown and clearance of the drug by the hepatic system after long-term presence in the body. The accumulation of PU24FCl in tumors is consistent with this agent's higher affinity for tumor versus normal tissue Hsp90 (Figure 2).

Pharmacodynamic Analysis

To probe the efficacy and safety of PU24FCl as an Hsp90 inhibitor in vivo, we used mice bearing MCF-7 breast cancer xenograft tumors. When compared to Her2-overexpressing breast cancer cell lines, MCF-7 shows only a modest response to 17AAG and is one of the cancer cell lines that evades apoptosis after Hsp90 inhibition or other pharmacological interferences ([32, 36]; Figure 4A). As pharmacodynamic markers, we followed the effect of PU24FCl on Hsp90 client proteins, such as Akt and Raf-1 kinases and the transmembrane tyrosine kinases Her2 and Her3, that are involved in the dysregulated growth and survival potential of MCF-7. When administered intraperitoneally, PU24FCl exhibited a dose-dependent effect on these Hsp90 client proteins, with no significant increase in benefit after 200 mg/kg (Figure 5C). One dose of 200 mg/kg PU24FCl caused a significant depletion of receptor tyrosine kinases (Her2, Her3, and Her4) as well as degradation and inactivation of Akt and Raf-1 in MCF-7 tumor xenografts, with a consistent relationship observed between its tumor accumulation profile and its effect on Hsp90 client proteins (Figures 5B and 5D). In contrast to 17AAG administration, no induction of Hsp70 was observed in tumors at the indicated times and doses (Figures 5C, 5D, and 5F). This is a somewhat surprising observation when one considers that, when it is administered in tissue culture to MCF-7 cells, PU24FCl does induce Hsp70 levels. It is not clear what the significance of Hsp70 induction in tumors might be, but it has been suggested that increased Hsp70 levels could interfere with the apoptotic potential of Hsp90 inhibitors [37]. Similar pharmacodynamic profile of PU24FCl was observed in mice bearing BT-474 breast cancer xenograft tumors, suggesting that the in vivo effects of the agent may not be restricted to one tumor type and that wide-range targeting of oncogenic transformation may also be achieved in vivo (Figure 5F). Our results also suggest that the broad-range anti-tumor activity should occur at similar doses, in concordance with this drug's affinity for tumor Hsp90. The in vivo degradation of Hsp90 client proteins by PU24FCl may translate to the usefulness of this agent or more potent agents of this class in several malignancies. The transmembrane tyrosine kinases whose degradation is induced by PU24FCl include Her2, Her3, and Her4 (Figures 5C, 5D, and 5F). The overexpression of these receptors has been associated with aggressive malignancies [38] and several therapeutic strategies targeting the receptors are now in various stages of clinical development [39]. These strategies act to block the activation or to inhibit the activity of the kinases (i.e., Herceptin and Iressa). "Kinase-dead" receptors can still function

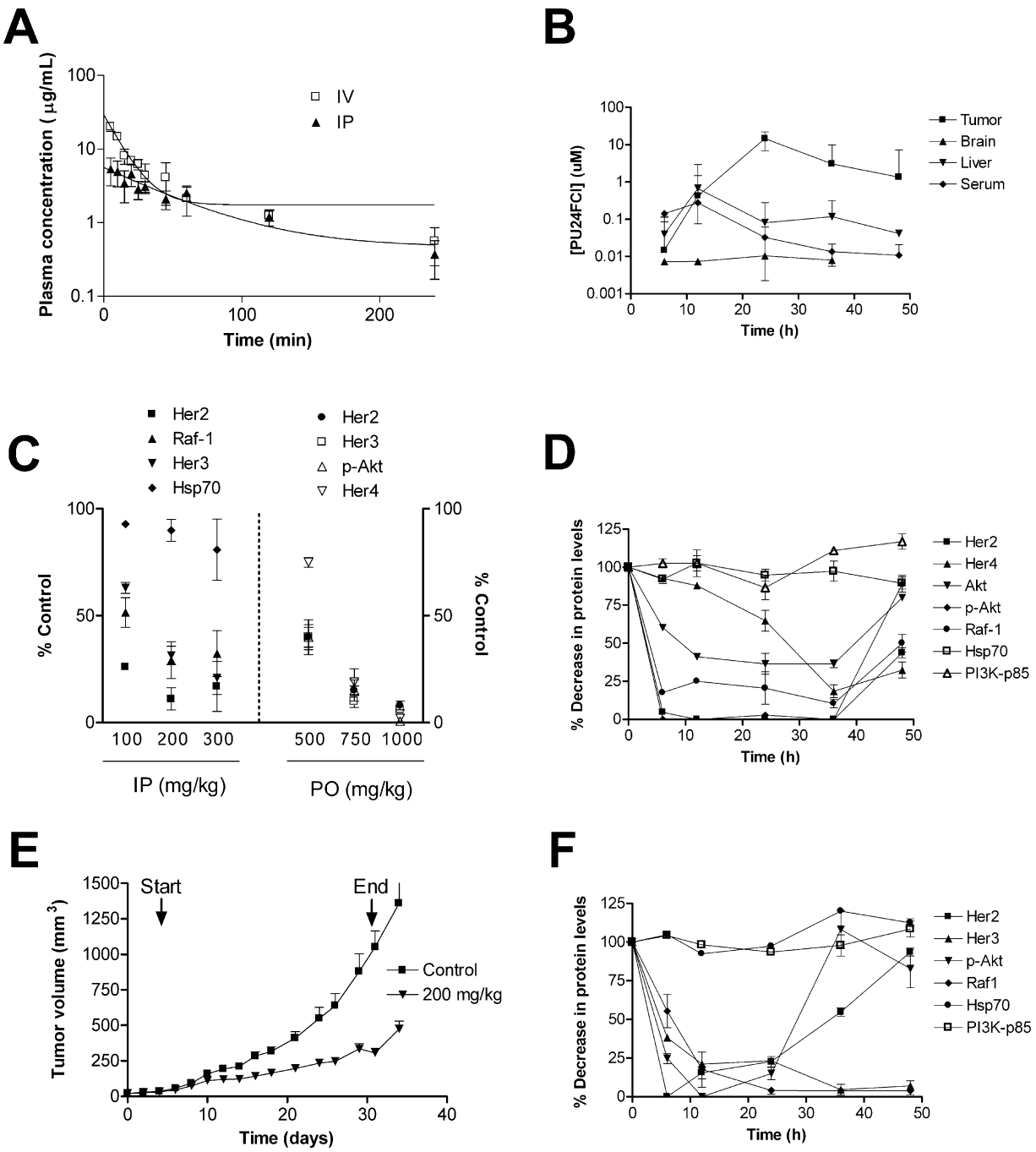

Figure 5. Analysis of PU24FCl In Vivo Administration

The high affinity of PU24FCl for tumor Hsp90 leads to accumulation in tumors with rapid clearance from normal tissue.

(A and B) Pharmacokinetic analysis of PU24FCl. (A) Early distribution (0 to 4 hr): mean plasma concentrations of PU24FCl versus time after single IP and IV bolus administration of 70 mg/kg PU24FCl to mice. The agent's concentration in serum was monitored from 0 to 4 hr after administration and showed rapid adsorption and distribution.

(B) Late distribution (6 to 48 hr): one dose of PU24FCl was administered intraperiotneally to MCF-7 (200 mg/kg) tumor-bearing mice for the indicated time periods. Mice were sacrificed, and tumors, organs, and serum were harvested. Drug distribution in tissue and serum was analyzed by LC-MS. In tumors, PU24FCl accumulated to concentrations found in vitro and induced all of its Hsp90-dependent anti-cancer effects while being rapidly cleared from organs.

(C–F) Pharmacodynamic effects of PU24FCl. (C) The effect of PU24FCl on Hsp90 clients is dose dependent. PU24FCl was administered intraperitoneally or by PO to MCF-7 tumor-bearing mice at the indicated doses. Mice were sacrificed at 8 hr (for IP) and 24 hr (for PO), and tumors were harvested. Tumors were processed, and protein levels were analyzed by Western blot. Data were presented as percent control = protein expression in treated mice/protein expression in control mice*100 and plotted against administered dose of PU24FCl. (D and F) Pharmacologically relevant concentrations can be achieved and maintained in several tumor types. One IP dose of PU24FCl was administered to MCF-7 (200 mg/kg) (D) and BT-474 (300 mg/kg) (F) tumor-bearing mice for the indicated time periods. Mice were sacrificed, and tumors were harvested (drug distribution in MCF-7 tumors is presented in panel [B]). Tumors were processed, and Hsp90 client protein levels were analyzed by Western blot. (E) Alternate-day administration of 200 mg/kg PU24FCl to MCF-7 tumor-bearing mice resulted in anti-tumor activity (approximately 70% inhibition) without visible toxicities. Mice (n=*5*) were treated for the indicated time period with an intraperitoneally administered dose, and tumor volume was measured as presented in the Experimental Procedures.

as a substrate for other receptors and non-receptor kinases and thus act as a docking protein capable of signaling. Thus, a more significant therapeutic outcome may result from degrading these oncoproteins via Hsp90 inhibition [40]. We have shown Akt and Raf-1 to be additional in vivo targets of PU24FCl (Figures 5C, 5D, and 5F). The Raf-MAPK pathway regulates cell proliferation, and differentiation and interference with the activity of proteins in this pathway is believed to be effective in cancer treatment [41]. In addition, Akt is an important regulator of cell proliferation and survival [42], and elevated Akt activity has been observed in tumors with mutations in PTEN, one of the most frequently mutated tumor suppressor genes [43, 44].

Based on our in vitro data, effects of PU24FCl on Hsp90 protein levels occurred alongside with growth arrest and induction of apoptosis at concentrations ranging from 1 to 10 μM. It is thus reasonable to believe that these doses may have effects in vivo on other cancer hallmarks dependent on Hsp90. Because a 200 mg/kg dose administered intraperitoneally resulted in 1–15 μM drug accumulated in tumors for at least 20 hr (Figure 5B), we tested this dose for inhibition of tumor growth. An alternate-day schedule of 200 mg/kg PU24FCl (no other dose or scheduling regiment was tried, and no efforts were made for optimization) was further studied for single-agent anti-tumor efficacy in the MCF-7 xenograft model. The study was conducted for 30 days to result in a 72% reduction in tumor burden in the treated group compared to the control (Figure 5E). No weight loss or visible internal change upon dissection was observed in the treated group (data not shown).

To explore whether this class of Hsp90 inhibitors could be ultimately tailored for oral administration, we tested the oral availability of PU24FCl. One dose of 500, −750 and −1000 mg/kg PU24FCl was administered by oral gavage (PO) to mice bearing MCF-7 xenograft tumors. Twenty-four hours after treatment, animals were sacrificed, tumors were analyzed, and a dose-dependent decline in Hsp90 client proteins was observed; the results were comparable to those obtained in the IP studies with this agent (Figure 5C). It is possible, in light of the cytostatic effect of Hsp90 inhibitors against some tumors, that repetitive dosing will be required, and oral availability may thus be an important factor for a successful clinical candidate of this action.

In conclusion, our results define a novel class of "drug-like" agents that target with similar potencies a broad spectrum of malignancies via specific inhibition of tumor Hsp90. As such, their activity would not be limited to a small subset of cancers. Administered alone or in combination with other agents, they would represent a novel therapeutic approach for the treatment of cancer patients with advanced disease.

Significance

A recent trend in cancer therapy has been to develop agents that "target" a single molecular alteration. However, most tumors are characterized by multiple growth-regulatory alterations, and these are specific to the type of tumor. Thus, drugs targeting one abnormality may be insufficient in reversing transformation and would be limited to use in a small subset of cancers. It has been suggested that one potential way to circumvent this problem is to target the machinery that allows most cancer cells to function with the burden of abnormalities they carry: the chaperone Hsp90. We have developed and validated a new generation of potent inhibitors that, by specific tumor Hsp90 inhibition, can unvaryingly target a broad range of cancers. As a result of their comprehensive targeting of oncogenic transformation, these agents might represent compelling new therapeutics.

Experimental Procedures

Syntheses of PU24FCl and GM-BODIPY were described elsewhere [26, 45].

Hsp90 Competition Assay

Fluorescence polarization measurements [45] were performed on an Analyst AD instrument (Molecular Devices, Sunnyvale, CA). Measurements were taken in black 96-well microtiter plates (Corning #3650). The assay buffer (HFB) contained 20 mM HEPES (K) (pH 7.3), 50 mM KCl, 5 mM $MgCl_2$, 20 mM Na_2MoO_4, and 0.01% NP40. Before each use, 0.1 mg/ml bovine γ globulin (BGG) (Panvera Corporation, Madison, WI) and 2 mM DTT (Fisher Biotech, Fair Lawn, NJ) were freshly added. For preparation of cell lysates, cellular membranes were frozen at −70°C so that membranes would be ruptured, and the cellular extract was dissolved in HFB with added protease and phosphotase inhibitors. Organs were harvested from a healthy mouse and homogenized in HFB. Saturation curves in which GM-BODIPY (5 nM) was treated with increasing amounts of cellular lysates were recorded. The amount of lysate that resulted in polarization (mP) readings corresponding to 20 nM recombinant Hsp90 α was chosen for the competition study. For the competition studies, each well contained 5 nM fluorescent GM, cellular lysate (amounts as determined above and normalized to total Hsp90 as determined by Western blot analysis with Hsp90 purified from HeLa cells [Stressgen# SPP-770] as a standard) and tested inhibitor (initial stock in DMSO) in a final volume of 100 μl. For liver, the amount of GM-BODIPY had to be increased because of high autofluorescence of the liver homogenate. The plate was left on a shaker at 4°C for 7 hr, and the FP values in mP were recorded. EC_{50} values were determined to be equal to the competitor concentration that displaced 50% of the fluorescent GM.

MutL ATPase Assay

ATP hydrolysis was determined at 37°C in reactions (20 μl) containing 20 mM Tris-HCl (pH 8.0), 90 mM KCl, 1 mM DTT, 4 μM d(T)100 (molecules), and 0.8 μM MutL. The effect of the inhibitors on ATP hydrolytic activity was determined by the addition of 5 mM PU24FCl or 17AAG. Hydrolysis was initiated by the addition of $[^{32}P]ATP{\cdot}(Mg^{2+})$ to prewarmed reactions to give a final concentration of 0.3 mM. At 10 min intervals, 2 μl samples were taken and quenched with 50 μl of 0.5 M EDTA (pH 8.0). The extent of ATP hydrolysis was determined by chromatography of 1 μl of the quenched sample on polyethyleneiminecellulose plates (EM Science) that were developed in 0.3 M K_3PO_4 (pH 7.0). Dried plates were phosphorimaged overnight and optically scanned with a STORM imager system, and data were analyzed with Imagequant software (Molecular Dynamics). Initial steady-state rates of hydrolysis were determined by least-squares analysis of the linear portion of the progress curve. One hundred percent activity corresponds to 8 mol ADT/min/mol of MutL. Inhibition of a panel of kinases was evaluated at Panlabs Pharmacology Services.

Cell Culture

The human cancer cell lines MCF-7, SKBr3, MDA-MB-468, BT-474, NCI-H69, NCI-N417, TSUPr1, Colo205, A549, A431, K562, and LNCaP were a gift from Dr. Neal Rosen, and Kasumi-1 and NB4 were from Dr. Steve Nimer (MSKCC). Cells were maintained in a 1:1

mixture of DME:F12 supplemented with 2 mM glutamine, 50 units/ml penicillin, 50 units/ml streptomycin, and 5%–10% heat-inactivated fetal bovine serum (Gemini Bioproducts) and incubated at 37°C, 5% CO_2.

Growth Assays

Growth inhibition studies were performed with the sulforhodamine B assay as previously described [16]. In summary, experimental cultures were plated in microtiter plates (Nunc). One column of wells was left without cells to serve as the blank control. Cells were allowed to attach overnight. The following day, growth medium having either drug or DMSO at twice the desired initial concentration was added to the plate in triplicate and was serially diluted at a 1:1 ratio in the microtiter plate. After 72 hr of growth, the cell number in treated versus control wells was estimated after treatment with 10% trichloroacetic acid and staining with 0.4% sulforhodamine B in 1% acetic acid. The IC_{50} was calculated as the drug concentration that inhibits cell growth by 50% compared with control growth. Normal prostate epithelial cells (PrEC) and human renal proximal tubular epithelial (RPTEC) cells were purchased preseeded in 96-well plates (Clonetics, CC-0088 and 3190, respectively). Upon receipt, cells were placed in a humidified incubator at 37°C, 5% CO_2 and allowed to equilibrate for 3 hr. Media were removed by suction and replaced with fresh media provided by the manufacturer. Cells were then treated with either drugs or DMSO for 72 hr, and the IC_{50} values were determined as described above.

Protein Assays

Cells were grown to 60%–70% confluence and exposed to drugs or DMSO vehicle for the indicated time periods. Lysates were prepared with 50 mM Tris (pH 7.4) and either 2% SDS or 1% NP-40 lysis buffer. Protein concentrations were determined with the BCA kit (Pierce) according to the manufacturer's instructions. Protein lysates (20–100 μg) were electrophoretically resolved on denaturing 7% SDS-PAGE, transferred to nitrocellulose membrane, and probed with the following primary antibodies: anti-Her2 (C-18), anti-Her3 (C-17), anti-Her4 (C-18), anti-Raf-1, hMet (C-28) (Santa Cruz), anti-ER (Stressgen Bioreagents), anti-β-actin (Sigma), anti-PI3K (p85) (Upstate Biotechnologies), anti-p53 (NeoMarkers), anti-cAbl (Oncogene), anti-AR (Pharmingen), anti-Akt, and anti-pAkt (Cell Signaling). Membranes were then incubated with a 1:5000 dilution of a peroxidase-conjugated corresponding secondary antibody. ECL (Amersham Life Science, Inc.) was performed according to the manufacturer's instructions. Blots were visualized by autoradiography, and the protein was quantified with BioRad Gel Doc 1000 software.

Flow Cytometry

Analysis of intracellular DNA content was performed on a FACScan flow cytometer (Becton Dickinson). Cells were trypsinized, harvested, and stained with 25 μg/ml EtBr in a citric buffer. Cells (20×10^5/sample) were analyzed at a rate of 100–200 cells/s. Data were analyzed with FlowJo software, and the percentage of cells in all cell cycle phases was determined as a ratio of the fluorescent area of the appropriate peaks to the total fluorescent area.

Differentiation of K562

Expression of the erythroid-specific surface marker GPA was determined by a previously described method [35]. In brief, 1×10^6 cells were incubated at 4°C for 30 min with 100 μl (10 μg/ml) of mouse antihuman GPA monoclonal antibody (Pharmingen). Next, cells were washed twice with ice-cold PBS to remove unbound antibody, resuspended in 10 μg/ml of FITC-labeled goat anti-mouse IgG (Wako), and incubated at 4°C for 30 min in the dark. The cells were then washed twice with ice-cold PBS and resuspended in 1% paraformaldehyde in PBS (pH 7.4). Mouse IgG1 (Wako) was used as an isotype-matched negative control for each sample. 10×10^3 events were analyzed for each sample by FACScan (Becton Dickinson).

Immunofluorescence

Differentiation

Cells were plated at 5000 cells/chamber slide (fibronectin-coated Lab-Tek 2-well chamber slides, Fisher Scientific) and seeded for 24 hr. Drug (10 μM) or vehicle was added for 48 hr, after which, for immunofluorescence, the slides were washed twice with ice-cold PBS and fixed with methanol and acetone solution (1:1) for 15 s. Fixed monolayers were washed with distilled water and blocked with 5% BSA in PBS solution. After blocking took place, cells were incubated with the primary antibody (anti-MFMG, Chemicon, 1:100 in 5% BSA in PBS) at 37°C and washed three times with 1% BSA in PBS; incubation with a rhodamine-labeled secondary antibody followed for 1 hr at 37°C.

Mitotic Block

Harvested cells were washed in PBS, fixed in methanol for 20 min at −20°C, washed again in PBS, and blocked for 30 min in PBS with 5% BSA. Cells were stained first with mouse monoclonal anti-α-tubulin (Sigma) and then with rhodamine-conjugated anti-mouse antibody as well as 1 μg/ml DAPI. Results were visualized, imaged, and quantified under confocal microscopy.

Animal Studies

Four- to 6-week-old *nu/nu* athymic female mice were obtained from the National Cancer Institute-Frederick Cancer Center and maintained in ventilated caging. Experiments were carried out under an Institutional Animal Care and Use Committee-approved protocol, and institutional guidelines for the proper and humane use of animals in research were followed. MCF-7 (5×10^6 cells) or BT-474 (1×10^7 cells) human mammary tumor cells were subcutaneously implanted in the right flank of *nu/nu* athymic mice via a 20 gauge needle and allowed to grow. Three days prior to tumor inoculation, 0.72 mg 17β-estradiol 90-day release pellets (Innovative Research of America, Sarasota, FL) were implanted subcutaneously in the left flank. For pharmacodynamic studies, tumors were allowed to reach 6–8 mm in diameter before treatment. Before administration, a solution of PU24FCl was prepared at the desired concentration in 50 μl vehicle (PBS:DMSO:EtOH at 1:1:1 ratio). At sacrifice, plasma, tumor, liver, and brain tissue were collected. A gross necropsy was performed on all mice. In experiments designed to define the pharmacodynamic effects of PU24FCl on Hsp90 client protein expression, mice ($n = 2$) with established tumors were treated with 200 mg/kg PU24FCl or with vehicle alone. At the time of sacrifice, serum was collected, and tumors and normal tissue were flash frozen. For protein analysis, tumors were homogenized in SDS lysis buffer (50 mM Tris [pH 7.4], 2% SDS). For pharmacokinetic analysis, plasma samples were obtained by retro-orbital puncture at the indicated times after the IP or IV administration of 70 mg/kg PU24FCl or vehicle alone. For quantitative HPLC analysis, tissue samples were homogenized in EtOH:H_2O (2:1) solution at a 1:3 w/v ratio. Concentrations of PU24FCl were determined by high-performance liquid chromatography-mass spectrometry (HPLC-MS) at the Analytical Core Facility of the Memorial Sloan-Kettering Cancer Center. The Agilent 1100 series (Agilent Instruments, Palo Alto, CA) was used for HPLC analysis with Sorbax SB-C8 column (i.d. 4×80 mm). The mobile phase consisted of acetonitrile (ACN) and 0.1% formic acid in water, and analysis was performed under gradient conditions from 45% to 65% ACN for 10 min and then 65% ACN for an additional 5 min at a flow rate of 0.4 ml/min. Serum samples were dissolved 1:2 (v/v) in MeOH, incubated at 4°C overnight, and centrifuged, and 20 μl of supernatant was injected into the column. The PU24FCl peak appeared at 7.5 min. For growth studies, tumors were allowed to reach 5 mm in diameter, and then animals were randomly divided into the treatment groups ($n = 5$). Mice were treated every other day with a dose of 200 mg/kg and then monitored for tumor progression. Tumor dimensions were measured every 2 days with vernier calipers, and tumor volumes were calculated with the formula $\pi/6 \times$ larger diameter $\times$ (smaller diameter)^2. Mice with established tumors of 4–5 mm in diameter were selected for study ($n = 5$ per treatment group). While on therapy, all mice received Augmentin (Amoxicillin/Clavulanate potassium; SmithKline Beecham) in their drinking water. Mice were sacrificed by CO_2 euthanasia.

Acknowledgments

This work was supported by the Susan G. Komen Foundation; the AACR and the Cancer Research and Prevention Foundation; the National Institutes of Health/National Cancer Institute; Mr. William H. Goodwin and Mrs. Alice Goodwin and the Commonwealth Cancer

Foundation for Research; the Experimental Therapeutics Center of Memorial Sloan-Kettering Cancer Center; and a generous donation by the Taub Foundation. We thank Drs. Mimnaugh, Neckers, Sausville, and Felts for useful suggestions in preparing the manuscript, Dr. Jacqueline She and Helen Haiying for technical expertise with in vivo experiments and William Tong for analytical expertise and suggestions.

Received: January 9, 2004
Revised: April 14, 2004
Accepted: April 20, 2004
Published: June 25, 2004

References

1. Buchdunger, E., Zimmermann, J., Mett, H., Meyer, T., Muller, M., Druker, B.J., and Lydon, N.B. (1996). Inhibition of the Abl protein-tyrosine kinase in vitro and in vivo by a 2-phenylaminopyrimidine derivative. Cancer Res. *56*, 100–104.
2. Druker, B.J., Talpaz, M., Resta, D.J., Peng, B., Buchdunger, E., Ford, J.M., Lydon, N.B., Kantarjian, H., Capdeville, R., Ohno-Jones, S., et al. (2001). Efficacy and safety of a specific inhibitor of the BCR-ABL tyrosine kinase in chronic myeloid leukemia. N. Engl. J. Med. *344*, 1031–1037.
3. Pietras, R.J., Fendly, B.M., Chazin, V.R., Pegram, M.D., Howell, S.B., and Slamon, D.J. (1994). Antibody to HER-2/neu receptor blocks DNA repair after cisplatin in human breast and ovarian cancer cells. Oncogene *9*, 1829–1838.
4. Vogel, C.L., Cobleigh, M.A., Tripathy, D., Gutheil, J.C., Harris, L.N., Fehrenbacher, L., Slamon, D.J., Murphy, M., Novotny, W.F., Burchmore, M., and Press, M. (2002). Efficacy and safety of trastuzumab as a single agent in first-line treatment of HER2-overexpressing metastatic breast cancer. J. Clin. Oncol. *20*, 719–726.
5. Shah, N.P., Nicoll, J.M., Nagar, B., Gorre, M.E., Paquette, R.L., Kuriyan, J., and Sawyers, C.L. (2002). Multiple BCR-ABL kinase domain mutations confer polyclonal resistance to the tyrosine kinase inhibitor imatinib (STI571) in chronic phase and blast crisis chronic myeloid leukemia. Cancer Cell *2*, 117–125.
6. Neckers, L. (2002). Hsp90 inhibitors as novel cancer chemotherapeutic agents. Trends Mol. Med. *8*, S55–S61.
7. Maloney, A., and Workman, P. (2002). HSP90 as a new therapeutic target for cancer therapy: the story unfolds. Expert Opin. Biol. Ther. *2*, 3–24.
8. Kamal, A., Thao, L., Sensintaffar, J., Zhang, L., Boehm, M.F., Fritz, L.C., and Burrows, F.J. (2003). A high-affinity conformation of Hsp90 confers tumour selectivity on Hsp90 inhibitors. Nature *425*, 407–410.
9. Neckers, L., Schulte, T.W., and Mimnaugh, E. (1999). Geldanamycin as a potential anti-cancer agent: its molecular target and biochemical activity. Invest. New Drugs *17*, 361–373.
10. Murakami, Y., Mizuno, S., Hori, M., and Uehara, Y. (1988). Reversal of transformed phenotypes by herbimycin A in src oncogene expressed rat fibroblasts. Cancer Res. *48*, 1587–1590.
11. Schulte, T.W., Akinaga, S., Soga, S., Sullivan, W., Stensgard, B., Toft, D., and Neckers, L.M. (1998). Antibiotic radicicol binds to the N-terminal domain of Hsp90 and shares important biologic activities with geldanamycin. Cell Stress Chaperones *2*, 100–108.
12. Supko, J.G., Hickman, R.L., Grever, M.R., and Malspeis, L. (1995). Preclinical pharmacological evaluation of geldanamycin as an antitumor agent. Cancer Chemother. Pharmacol. *36*, 305–315.
13. Schulte, T.W., and Neckers, L.M. (1998). The benzoquinone ansamycin 17-allylamino-17-demethoxygeldanamycin binds to Hsp90 and shares important biologic activities with geldanamycin. Cancer Chemother. Pharmacol. *42*, 273–279.
14. Solit, D.B., Zheng, F.F., Drobnjak, M., Munster, P.N., Higgins, B., Verbel, D., Heller, G., Tong, W., Cordon-Cardo, C., Agus, D.B., et al. (2002). 17-Allylamino-17-demethoxygeldanamycin induces the degradation of androgen receptor and HER-2/neu and inhibits the growth of prostate cancer xenografts. Clin. Cancer Res. *8*, 986–993.
15. Bagatell, R., Khan, O., Paine-Murrieta, G., Taylor, C.W., Akinaga, S., and Whitesell, L. (2001). Destabilization of steroid receptors by heat shock protein 90-binding drugs: a ligand-independent approach to hormonal therapy of breast cancer. Clin. Cancer Res. *7*, 2076–2084.
16. Kelland, L.R., Sharp, S.Y., Rogers, P.M., Myers, T.G., and Workman, P. (1999). DT-diaphorase expression and tumor cell sensitivity to 17-allyamino-17-demethoxygeldanamycin, an inhibitor of heat shock protein *90*. J. Natl. Cancer Inst. *91*, 1940–1949.
17. Prodromou, C., Roe, S.M., Piper, P.W., and Pearl, L.H. (1997). A molecular clamp in the crystal structure of the N-terminal domain of the yeast Hsp90 chaperone. Nat. Struct. Biol. *6*, 477–482.
18. Bergerat, A., de Massy, B., Gadelle, D., Varoutas, P.C., Nicolas, A., and Forterre, P. (1997). An atypical topoisomerase II from Archaea with implications for meiotic recombination. Nature *386*, 414–417.
19. Mushegian, A.R., Bassett, D.E., Jr., Boguski, M.S., Bork, P., and Koonin, E.V. (1997). Positionally cloned human disease genes: patterns of evolutionary conservation and functional motifs. Proc. Natl. Acad. Sci. USA *94*, 5831–5836.
20. Dutta, R., and Inouye, M. (2000). GHKL, an emergent ATPase/kinase superfamily. Trends Biochem. Sci. *25*, 24–28.
21. Prodromou, C., Roe, S.M., O'Brien, R., Ladbury, J.E., Piper, P.W., and Pearl, L.H. (1997). Identification and structural characterization of the ATP/ADP-binding site in the Hsp90 molecular chaperone. Cell *90*, 65–75.
22. Obermann, W.M., Sondermann, H., Russo, A.A., Pavletich, N.P., and Hartl, F.U. (1998). In vivo function of Hsp90 is dependent on ATP binding and ATP hydrolysis. J. Cell Biol. *143*, 901–910.
23. Panaretou, B., Prodromou, C., Roe, S.M., O'Brien, R., Ladbury, J.E., Piper, P.W., and Pearl, L.H. (1998). ATP binding and hydrolysis are essential to the function of the Hsp90 molecular chaperone in vivo. EMBO J. *17*, 4829–4836.
24. Chiosis, G., Timaul, M.N., Lucas, B., Munster, P.N., Zheng, F.F., Sepp-Lorenzino, L., and Rosen, N. (2001). A small molecule designed to bind to the adenine nucleotide pocket of Hsp90 causes Her2 degradation and the growth arrest and differentiation of breast cancer cells. Chem. Biol. *8*, 289–299.
25. Chiosis, G., Lucas, B., Huezo, H., Solit, D., Basso, A., and Rosen, N. (2003). Development of purine-scaffold small molecule inhibitors of Hsp90. Curr. Cancer Drug Targets *3*, 371–376.
26. Chiosis, G., Lucas, B., Shtil, A., Huezo, H., and Rosen, N. (2002). Development of a purine-scaffold novel class of Hsp90 binders that inhibit the proliferation of cancer cells and induce the degradation of Her2 tyrosine kinase. Bioorg. Med. Chem. *10*, 3555–3564.
27. Lipinski, C.A., Lombardo, F., Dominy, B.W., and Feeney, P.J. (1997). Experimental and computational approaches to estimate solubility and permeability in drug discovery and developmental settings. Adv. Drug Deliv. Rev. *23*, 3–25.
28. Veber, D.F., Johnson, S.R., Cheng, H.Y., Smith, B.R., Ward, K.W., and Kopple, K.D. (2002). Molecular properties that influence the oral bioavailability of drug candidates. J. Med. Chem. *45*, 2615–2623.
29. Chiosis, G., Huezo, H., Rosen, N., Mimnaugh, E., Whitesell, L., and Neckers, L. (2003). 17AAG: low target binding affinity and potent cell activity—finding an explanation. Mol. Cancer Ther. *2*, 123–129.
30. Ban, C., Junop, M., and Yang, W. (1999). Transformation of MutL by ATP binding and hydrolysis: a switch in DNA mismatch repair. Cell *97*, 85–97.
31. Spampinato, C., and Modrich, P. (2000). The MutL ATPase is required for mismatch repair. J. Biol. Chem. *275*, 9863–9869.
32. Munster, P.N., Marchion, D.C., Basso, A.D., and Rosen, N. (2002). Degradation of HER2 by ansamycins induces growth arrest and apoptosis in cells with HER2 overexpression via a HER3, phosphatidylinositol 3′-kinase-AKT-dependent pathway. Cancer Res. *62*, 3132–3137.
33. Munster, P.N., Srethapakdi, M., Moasser, M.M., and Rosen, N. (2001). Inhibition of heat shock protein 90 function by ansamycins causes the morphological and functional differentiation of breast cancer cells. Cancer Res. *61*, 2945–2952.
34. Burger, P.E., Dowdle, E.B., Lukey, P.T., and Wison, E.L. (1994).

Basic fibroblast growth factor antagonizes transforming growth factor beta-mediated erythroid differentiation in K562 cells. Blood *83*, 1808–1812.

35. Shiotsu, Y., Neckers, L.M., Wortman, I., An, W.G., Schulte, T.W., Soga, S., Murakata, C., Tamaoki, T., and Akinaga, S. (2000). Novel oxime derivatives of radicicol induce erythroid differentiation associated with preferential G(1) phase accumulation against chronic myelogenous leukemia cells through destabilization of Bcr-Abl with Hsp90 complex. Blood *96*, 2284–2291.
36. Munster, P.N., Basso, A., Solit, D., Norton, L., and Rosen, N. (2001). Modulation of Hsp90 function by ansamycins sensitizes breast cancer cells to chemotherapy-induced apoptosis in a RB- and schedule-dependent manner. Clin. Cancer Res. *8*, 2228–2236.
37. Maloney, A., Clarke, P.A., and Workman, P. (2003). Genes and proteins governing the cellular sensitivity to HSP90 inhibitors: a mechanistic perspective. Curr. Cancer Drug Targets *3*, 331–341.
38. Slamon, D.J., Godolphin, W., Jones, L.A., Holt, J.A., Wong, S.G., Keith, D.E., Levin, W.J., Stuart, S.G., Udove, J., Ullrich, A., et al. (1989). Studies of the *HER-2/neu* proto-oncogene in human breast and ovarian cancer. Science *244*, 707–712.
39. Mendelsohn, J., and Baselga, J. (2000). The EGF receptor family as targets for cancer therapy. Oncogene *19*, 6550–6565.
40. Citri, A., Alroy, I., Lavi, S., Rubin, C., Xu, W., Grammatikakis, N., Patterson, C., Neckers, L., Fry, D.W., and Yarden, Y. (2002). Drug-induced ubiquitylation and degradation of ErbB receptor tyrosine kinases: implications for cancer therapy. EMBO J. *21*, 2407–2417.
41. Hilger, R.A., Scheulen, M.E., and Strumberg, D. (2002). The Ras-Raf-MEK-ERK pathway in the treatment of cancer. Onkologie *25*, 511–518.
42. Chang, F., Lee, J.T., Navolanic, P.M., Steelman, L.S., Shelton, J.G., Blalock, W.L., Franklin, R.A., and McCubrey, J.A. (2003). Involvement of PI3K/Akt pathway in cell cycle progression, apoptosis, and neoplastic transformation: a target for cancer chemotherapy. Leukemia *17*, 590–603.
43. Graff, J.R. (2002). Emerging targets in the AKT pathway for treatment of androgen-independent prostatic adenocarcinoma. Expert Opin. Ther. Targets *6*, 103–113.
44. Knobbe, C.B., Merlo, A., and Reifenberger, G. (2002). Pten signaling in gliomas. Neuro-oncol. *4*, 196–211.
45. Llauger-Bufi, L., Felts, S.F., Huezo, H., Rosen, N., and Chiosis, G. (2003). Synthesis of novel fluorescent probes for the molecular chaperone Hsp90. Bioorg. Med. Chem. Lett. *13*, 3975–3978.